DOI: 10.1002/stco.202400043

Batuhan Der, František Wald, Martin Vild

ARTICLE

Numerical design calculation of flush endplate connections at elevated temperatures

The fire design of bolted connections is a critical aspect of structural fire engineering, as the failure of steel connections under fire conditions can compromise the entire structure. This paper presents numerical design calculations of flush endplate connections using the component-based finite-element method (CBFEM) at elevated temperatures. The CBFEM models are developed and validated against experimental data, focusing on load-rotation behaviour, connection resistance, and failure modes under thermal stress. By integrating the component method with finite-element analysis, CBFEM provides a robust framework for simulating the behaviour of steel connections in fire. Additionally, the method is verified against Eurocode design specifications for further validation. The results demonstrate that CBFEM is a reliable and accurate approach for the fire design of bolted steel connections at elevated temperatures, offering precise predictions of connection performance and failure mechanisms.

Keywords flush endplate connections; fire resistance; component-based finite-element method; numerical calculation

1 Introduction

The failure of steel connections may result in the collapse of the entire building at elevated temperatures due to their influences on internal forces distribution and overall deformation. Hence, the resistance of steel connections at elevated temperatures should be accurately predicted to understand the structural fire performance. Wald et al. [1] conducted the Cardington fire experiments to understand the effect of connections on the mechanical behaviour of steel structures at elevated temperatures. The connection types studied in the Cardington tests are endplate and finplate connections.

Flush endplate connections are commonly used in steel structures, thanks to their easy fabrication, good performance, and low cost [2]. The elastic and plastic deformations of the connection components including the endplate in bending, the bolts in tension, the bending of the column flange, and the column web in shear govern the nonlinear behaviour of the flush endplate connections [3]. Several experimental studies were performed to investigate the mechanical response of flush endplate connections at ambient and elevated temperatures [4–9]. Leston Jones et al. [4] performed a single test at ambient and five tests at elevated temperatures to develop the moment–rotation characteristics of steel flush endplate connections. Yu et al. [5] reported a series of tests on flush endplate connections subjected to combinations of tying force (normal to the column face) and shear force (parallel to the column face) at elevated temperatures. Three tests at elevated temperatures were carried out by Li et al. [6] to investigate the temperature distribution, load-carrying capacity, and failure mode of the flush endplate composite joints. Ataei et al. [7] performed an experimental study on four full-scale sustainable flush endplate semi-rigid beam-to-column joints with deconstructable bolted shear connectors. The study determined the failure modes and to characterize the moment and rotation capacities, moment–rotation relationships and ductilities of this new deconstructable composite system. Khonsari et al. [8] conducted a fire test to assess the mechanical behaviour of bare steel flush endplate connections with relatively low thickness in a 3D frame at elevated temperatures. They observed several failure modes including bolt fracture, bolt thread stripping, and large inelastic deformation of the endplates. The adoption of thin endplates increased the rotational capacity of the connections. Lu et al. [9] conducted an experimental study on high-strength Q690 steel flush endplate connections (Q690-FEC) at ambient and elevated temperatures to investigate the bending capacity and failure modes of flush endplate connections. Fire tests help structural fire engineers to understand better the mechanical behaviour of steel connections at elevated temperatures. However, the fire tests are not feasible to conduct for all steel connection types due to the limitations in furnace size and experimental costs.

The fire resistance of steel connections may be evaluated by analytical and finite-element models. EN 1993-1-8 [10] standardizes the component-based method to analyse the steel connections at ambient temperatures. The component-based method may be used to predict the fire behaviour of steel connections using the reduction factors for structural steel, bolts, and welds proposed in EN 1993-1-2 [11]. Numerical studies are important tools for understanding the mechanical response of steel connections at elevated temperatures comparing prescriptive and performance-based approaches [12] to the design of steel connections in fire conditions. Both prescriptive

and performance-based approaches use finite-element methods (FEMs). The prescriptive approach simulates the mechanical behaviour of steel connections exposed to standardized fire exposure. In contrast, experimental fire scenarios or real fire data might be used to validate the performance-based models. Several numerical models [13–17] have been generated to model the flush endplate connections at elevated temperatures. Al-Jabri et al. [13] developed a finite-element model using 3D solid elements to study the responsive flush endplate bare steel connections and establish the moment–rotation characteristics of the connections under the combined loading of a concentrated force at elevated temperatures. Tran [16] developed a model for predicting the moment–rotation–temperature relationship of semi-rigid cruciform flush endplate connections in the fire. Numerical models can be classified as numerical simulation (NS) and numerical design calculation (NDC) [18]. NS is an advanced numerical model that may utilize the measured material properties, geometrical imperfections, and residual stresses in order to fit the real mechanical behaviour of structural members. The numerical models mentioned in this paragraph are good examples of NS. However, the generation of a validated NS is not a feasible method at the fire design level due to the high computational cost. The NDC uses design material models such as a bilinear material curve with von Mises yield criterion, standard safety factors, and a reduced number of finite elements and nodes compared to NS. These simplifications may decrease the computational effort and make the model more practicable at the design level. The component-based finite-element method (CBFEM) model is a special type of NDC to design steel connections at ambient and elevated temperatures. Fig. 1 indicates the material model for steel used in NS. Validation and verification are important steps to ensure the accuracy and reliability of a finite-element model. Der et al. [19–21] validated and verified the CBFEM to predict bolted fire resistance and failure modes of bolted lap joints, finplate connections, and T-stubs at elevated temperatures.

This paper presents a CBFEM model to model the behaviour of flush endplate connections at elevated temperatures. The CBFEM is validated using the experimental results, specifically focusing on load–rotation curves and failure modes of tested connections. The verification study is performed to analyse the reliability of the CBFEM for steel connection design. To verify the model, the T-stub specimen is created using the tested specimens with the top bolt-row. The CBFEM results for the T-stub are compared with the analytical model (AM) presented in EN 1993-1-8 [10]. In the CBFEM model, the degradation of material properties for steel connection components is considered using the reduction factors proposed in EN 1993-1-2 [11]. The failure mode for steel plates reaches 5 % plastic limit strain recommended in EN 1993-1-5 [22]. Parametric studies are conducted to analyse the influence of different parameters such as the plastic limit strain of steel, bolt elongation, and bolt diameter on the mechanical response of flush endplate connections at elevated temperatures.

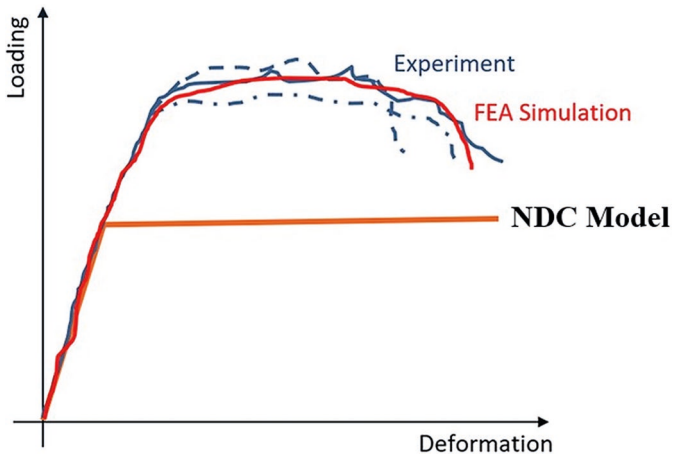

Fig. 1 Material model of structural steel in NDC model

2 Numerical calculation

Two numerical methods presented in the prEN 1993-1-14 [18] are NS and NDC. In this study, the flush endplate connections are analysed by NDC using the CBFEM.

2.1 CBFEM

The CBFEM is a method to analyse and design connections of steel structures. It is a combination of the component method and the FEM. The stresses, strains, and internal forces are calculated using the advantages of the FEM to check the individual components according to design specifications [10, 11, 22]. The CBFEM splits the entire joint into separated components including steel plates, welds, and bolts. The CBFEM model of steel connections may consist of plates, bolts, anchors, and welds. All plates are meshed with four-node quadrangle shell elements. Deformations of the element are divided into the membrane and the flexural components. Bolts are represented by nonlinear springs with their properties based on design codes. The bolt in tension is described by the spring with its axial initial stiffness, design resistance, initialization of yielding, and deformation capacity, as shown in Fig. 2. The initial axial stiffness is derived analytically in the guideline VDI [23] and Agerskov [24] as follows.

$$D_{\mathrm{Lb}} = \frac{L_s + 0.4 d_b}{E_\theta A_{\mathrm{ss}}} \tag{1}$$

$$A_{\mathrm{pp}} = \frac{0.75 D_H (L_w - D_H)}{D_{\mathrm{W1}}^2 - D_{\mathrm{W2}}^2} \tag{2}$$

$$A_{\mathrm{P1}} = \frac{\pi}{4}\left(D_H^2 - D_{\mathrm{W1}}^2\right) \tag{3}$$

$$A_{\mathrm{P2}} = \frac{1}{2}\left(D_{\mathrm{W2}}^2 - D_H^2\right)\tan^{-1} A_{\mathrm{pp}} \tag{4}$$

$$A_P = A_{\mathrm{P1}} + A_{\mathrm{P2}} \tag{5}$$

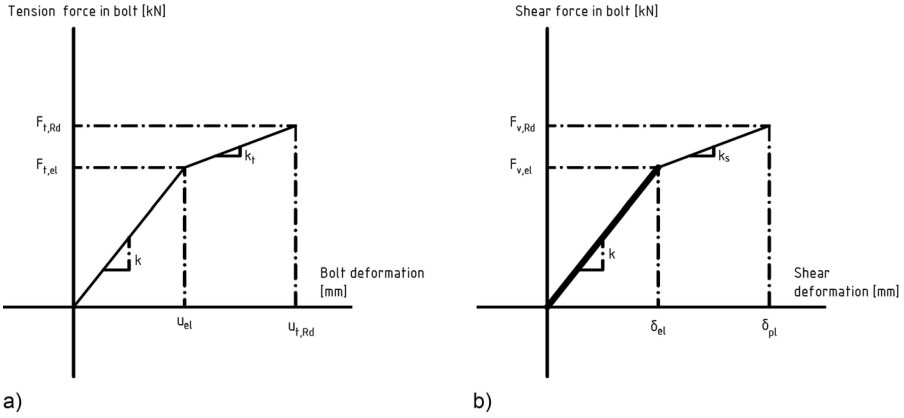

Fig. 2 The load–deformation behaviour of bolts in tension (la) and in shear (rb)

$$D_{\mathrm{LW}} = \frac{L_W}{E_\theta A_P} \tag{6}$$

$$k = \frac{1}{D_{\mathrm{LB}} + D_{\mathrm{LW}}} \tag{7}$$

where d_b is bolt diameter, D_H is bolt head diameter, D_{w1} and D_{w2} are washer inner and outer diameter, L_W is washer thickness, L_s is bolt grip length, A_{ss} is bolt gross area, and E is the temperature-dependent modulus of elasticity. The force–deformation diagram for bolts in tension is constructed using the following equations.

$$k_t = c_1 k \tag{8}$$

$$F_{\mathrm{t,el}} = \frac{F_{\mathrm{t,Rd}}}{c_1 c_2 - c_1 + 1} \tag{9}$$

$$u_{\mathrm{el}} = \frac{F_{\mathrm{t,el}}}{k} \tag{10}$$

$$u_{\mathrm{t,Rd}} = c_2 u_{\mathrm{el}} \tag{11}$$

$$c_1 = \frac{f_{\mathrm{ub},\theta} - f_{\mathrm{yb},\theta}}{0.25\, A E_\theta - f_{\mathrm{yb},\theta}} \tag{12}$$

$$c_2 = \frac{A E_\theta}{4 f_{\mathrm{yb},\theta}} \tag{13}$$

where $F_{t,\mathrm{Rd}}$ is the bolt design resistance in tension, $f_{\mathrm{yb},\theta}$ is the yield strength of a bolt, $f_{\mathrm{ub},\theta}$ is the ultimate strength of bolt, and A is elongation after fracture. Fig. 2 presents the characteristics of bolt behaviour in shear. The initial stiffness and the design resistance of a bolt in shear is defined by the following formulae.

$$k_{\mathrm{el}} = \frac{1}{\frac{1}{k_{11}} + \frac{1}{k_{12}}} \tag{14}$$

$$k_{11} = \frac{8 d_b^2 f_{\mathrm{ub},\theta}}{d_{\mathrm{M16}}} \tag{15}$$

$$k_{12} = 12 k_t d_b f_{\mathrm{up},\theta} \tag{16}$$

$$k_t = \left(2.5, \frac{1.5 t_{\mathrm{min}}}{d_{\mathrm{M16}}}\right) \tag{17}$$

$$k_s = \frac{k_{\mathrm{el}}}{1000} \tag{18}$$

where d_b is the bolt diameter, $f_{\mathrm{ub},\theta}$ is the temperature-dependent bolt ultimate strength, d_{M16} is the diameter of the reference bolt M16, $f_{\mathrm{up},\theta}$ is the temperature-dependent ultimate strength of the connected plate, and t_{min} is the minimum thickness of the connected plate. The spring for bolt in shear has a bilinear force deformation behaviour response. The characteristics of load deformation in shear can be calculated as follows.

$$F_{\mathrm{v,el}} = 0.999 F_{\mathrm{v,Rd}} \tag{19}$$

$$\delta_{\mathrm{pl}} = \delta_{\mathrm{el}} \tag{20}$$

where δ_{pl} and δ_{el} are bolt in shear plastic and elastic deformation, $F_{v,\mathrm{el}}$ is bolt shear elastic resistance, and $F_{v,\mathrm{Rd}}$ is bolt shear resistance. The effect of temperature on the elastic modulus, yield strength, and ultimate strength of bolts and structural steel is represented by the reduction factors proposed in EN 1993-1-2 [11]. Therefore, the temperature-dependent parameters introduced in previous equations are multiplied by the reduction factors at the targeted temperature.

There are several parameters mentioned in the equations above. The required parameters for building the force–deformation behaviour of the bolts in tension and shear are listed in Tab. 1. These design values are taken from the ISO 898 [25]. These parameters depend on the bolt grade.

Tab. 1 Bolt parameters in tension

Bolt grade	A [%]	c_1 [−]	c_2 [−]
4.8	14	0.011	21.6
5.6	20	0.02	35
6.8	8	0.032	8.8
8.8	12	0.03	9.5
10.9	9	0.026	5

In NS, the material properties from coupon tests are generally used to simulate the behaviour of steel connections. However, the NDC models use simplified material curves based on design specifications. The CBFEM models, the plates, with elastic–plastic material shows a nominal yielding plateau slope $\tan^{-1}$ (E/1000) according to EN 1993-1-5 [22]. The von Mises yield criterion governs the material's response under stress. It is considered to exhibit elastic behaviour until it reaches the design yield strength (f_{yd}). EN 1993-1-5 recommends the value of a 5 % plastic limit strain for simulating the behaviour of plates. Fig. 3 indicates the theoretical true and engineering stress–strain curves and the material model utilized in the CBFEM.

CBFEM employs the standard penalty method to simulate contact between plates. Penalty stiffness is introduced in case of penetration between a node and the opposing plate. A heuristic algorithm governs the adjustment of penalty stiffness throughout the nonlinear iteration, enhancing convergence. The solver autonomously identifies penetration points and addresses the distribution of contact forces between the penetrated node and nodes on the opposing plate.

CBFEM is a method implemented within IDEA StatiCa Connection [26] to model and analyse steel connections. When analysing steel frames or girder structures, the joints between members are treated as massless points. Equilibrium equations are formulated at these joints, and the internal forces at the beam ends are calculated after solving the entire structure. The resultant of forces from all members in the joint is 0, ensuring the joint remains in equilibrium. IDEA StatiCa Connection [26] may conduct two types of analyses: geometrically linear analysis with material and contact nonlinearities for stress and strain analysis and eigenvalue analysis to determine the possibility of buckling.

2.2 Failure modes

The CBFEM models each component of the connection, plates, bolts, welds, and anchors, as individual elements, capturing their interaction under applied loads. There are mainly three potential failure modes: bolt failure, weld failure, and plate failure. Bolt failure includes shear, tension, and bearing. Interaction between the axial and the shear force can be introduced directly in the analysis model. In the CBFEM, the bolt with its behaviour in tension, shear, and bearing is the component described by the dependent nonlinear springs. The CBFEM method evaluates the applied loads on the bolts and compares them with their capacities, calculated based on EN 1993-1-2 [11] and EN 1993-1-8 [10]. If the applied loads exceed the bolt capacities, the analysis cannot proceed.

Plate failure according to the CBFEM in IDEA StatiCa Connection [26] is analysed as part of the connection design. The software calculates stresses (e.g., normal, shear) and strains in the plate under various loading conditions. Plate failure occurs when the stress in the plate exceeds the yield strength of the material. The failure of the plate is generally considered when the equivalent plastic strain exceeds a certain threshold. The 5% limit is a suggested value but can be modified by the user in the code setup within IDEA StatiCa Connection.

2.3 Mesh sensitivity study

A mesh sensitivity study is a critical issue for finite-element modelling. To assess the accuracy of the NDC and optimize the computational cost, a mesh sensitivity study is performed. The study shows that the coarse mesh predicts higher resistance than the fine mesh. Fig. 4 shows the influence of the number of elements on the connection resistance. As the mesh becomes finer, the predicted resistance converges to a stable resistance value. However, increasing the number of mesh elements leads to higher computational costs. Therefore, the optimized element number is selected as 30 to divide the plates in CBFEM.

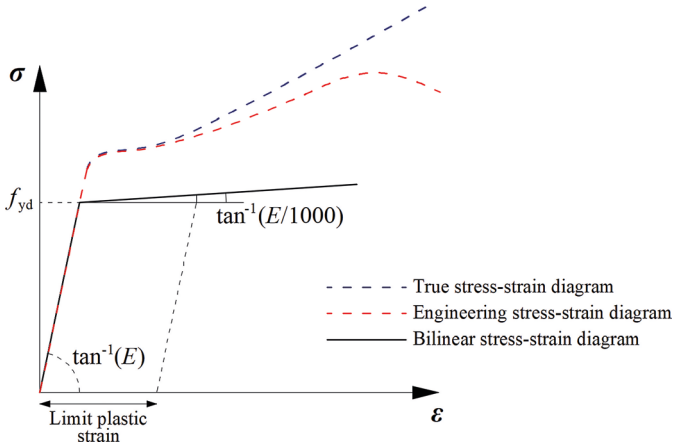

Fig. 3 Material models used in FEMs

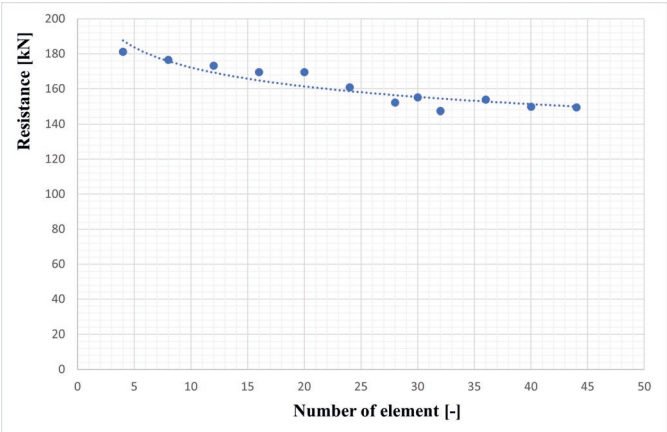

Fig. 4 Mesh sensitivity study

3 Verification

Verification is an essential step in finite-element modelling to ensure the reliability of the numerical results. The proposed numerical model can be verified utilizing the AMs or the validated numerical model according to prEN 1993-1-14 [18]. Eurocode suggests that an equivalent T-stub in tension may be used to model the resistance of column flange in bending and endplate bending in bolted connections. The EN 1993-1-8 [10] considers the area of the endplate connection in tension as a T-stub. There are three failure modes for the T-stub, as shown in Fig. 5. In failure mode 1, the flanges completely yield, failure mode 2 is the yielding of flanges accompanied by failure of the bolts, and bolt failure is failure mode 3.

The force at each bolt-row should not exceed the design resistance determined considering only that individual bolt-row. Therefore, the T-stub is cut from the test specimen using the top bolt-row. The geometrical dimensions of the T-stub specimen and the assembly of the T-stub in CBFEM are indicated in Fig. 6. The pitch distance refers to the horizontal distance between the centre of bolt holes and equals 90 mm.

The tension strength of bolted T-stubs that failed by flange yielding at elevated temperatures could be calculated as follows.

$$F_{T,1,Rd,\theta} = \frac{4M_{pl,1,Rd,\theta}}{m} \tag{21}$$

$$M_{pl,1,Rd,\theta} = 0.25 \sum l_{eff,1} t_f^2 f_{y,\theta} / M0 \tag{22}$$

where $M0 = 1.0$ is the partial factor provided by Eurocode and $f_{y,\theta}$ is the yield strength of the T-stub flange at high temperature θ. $M_{pl,1,Rd,\theta}$ is the bending strength of the T-stub flange at high temperature θ. $l_{eff,1}$ is the total length of the yielding line of the T-stub. EN 1993-1-8 [10] provides equations to calculate the tension strength of the bolted T-stub fails by flange yielding accompanied by bolt failure at ambient temperatures.

$$F_{T,2,Rd,\theta} = \frac{2M_{pl,2,Rd,\theta} + n \sum F_{t,Rd,\theta}}{m + n} \tag{23}$$

$$M_{pl,2,Rd,\theta} = 0.25 \sum l_{eff,2} t_f^2 f_{y,\theta} / \gamma_{M0} \tag{24}$$

$$F_{t,Rd,\theta} = \frac{k_2 f_{ub,\theta} A_s}{\gamma_{M2}} \tag{25}$$

where e is the distance between the axis of the bolt hole and the edge of the T-stub flange, l_{eff} is the total length of the yielding line of T-stubs, $f_{ub,\theta}$ is the ultimate tensile strength of a bolt at high temperature θ ($f_{ub,20kb\theta}$), $M_{pl,2,Rd,\theta}$ is the bending strength of the T-stub flange at high temperature θ. A_s is the effective cross-section area of a bolt, the coefficients $\gamma_{M2} = 1.25$ and $k_2 = 0.9$ are provided by Eurocode.

$$l_{eff,1,2} = \boldsymbol{min}(l_{eff,cp}, l_{eff,np}, l_{eff,bp}) \tag{26}$$

$$l_{eff,cp} = 2\pi m \text{ circular pattern} \tag{27}$$

$$l_{eff,np} = 4\, m + 1.25\, n \text{ non-circular pattern} \tag{28}$$

$$l_{eff,bp} = b \text{ beam pattern} \tag{29}$$

The tension strength of bolt failure at elevated temperatures could be calculated by

$$F_{T,3,Rd,\theta} = \sum F_{t,Rd,\theta} \tag{30}$$

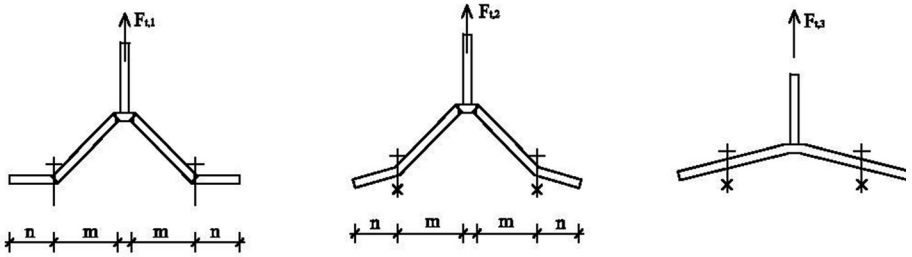

1. Mode 2. Mode 3. Mode

Fig. 5 Failure modes for T-stubs

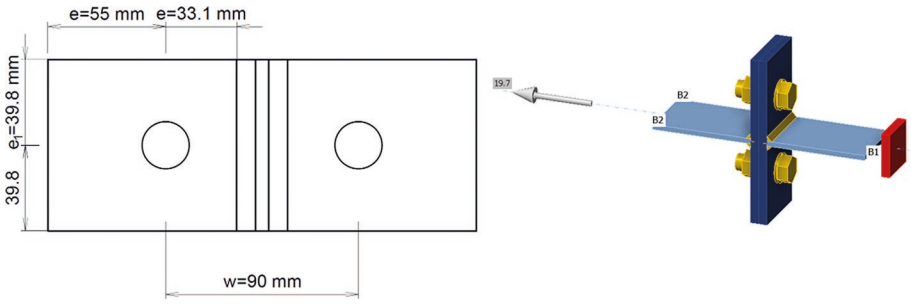

Fig. 6 Geometrical dimension and assembly of T-stub

$$F_{T,Rd,\theta}=\min(F_{T,1,Rd,\theta},F_{T,2,Rd,\theta},F_{T,3,Rd,\theta})\frac{\gamma_{M2}}{\gamma_{M,fi}} \qquad (31)$$

where $F_{t,Rd,\theta}$ is the tension resistance of bolts at temperature θ and $\gamma_{M,fi}$ is the partial safety factor for fire conditions [=1.0]. Fig. 7 shows the comparison values for the resistance of T-stubs calculated by the CBFEM model and AM. Generally, the resistance from AM is higher than the resistance from the CBFEM. The analysed T-stub specimens were prepared based on the test specimens loaded with 45°. The geometrical characteristics of the verification study are explained in Section 4. The resistance of the T-stubs was calculated at ambient temperature, 450, 550, and 650 °C. Finally, the thickness of the T-stub flange was changed from 10 to 8 and 15 mm at 550 °C.

4 Validation

In order to understand the mechanical response of flush endplate connections at high temperatures, the study of Yu et al. [5] on bolted beam-to-column connections was selected since several failure modes were observed. This section presents the validation of the CBFEM model using experimental results based on the requirements described by Wald et al. [27]. The CBFEM model is validated in terms of the load–deformation curves and failure modes.

4.1 Test description

The connection consists of a UC254×89 column and a UB305×165×40 beam. In all the tests, the steel column and the steel beams were made of S355 and S275, respectively. A typical endplate connection was designed with three rows of bolts in accordance with UK design recommendations [28]. The 325 mm deep × 200 mm width flush endplates made of grade S275 were connected to the beams with M20 Grade 8.8 bolts. The specimens were tested under steady-state conditions. The characteristics of test specimens are presented in Fig. 8. The plate thickness used in tests varied from 8, 10, and 15 mm. The load is applied to the test specimens through a special connector with an angle described in Tab. 2. The test specimens were loaded with three different angles 35°, 45°, and 55° at room temperature, 450, 550, and 650 °C. The test specimens used to validate the CBFEM model include three rows of bolts, as shown in Fig. 8. At 20 and 450 °C, the test specimens with three-bolt rows and 10 mm plate thickness failed due to the endplate fracture. At 550 and 650 °C, the bolt failure was observed with very ductile behaviour.

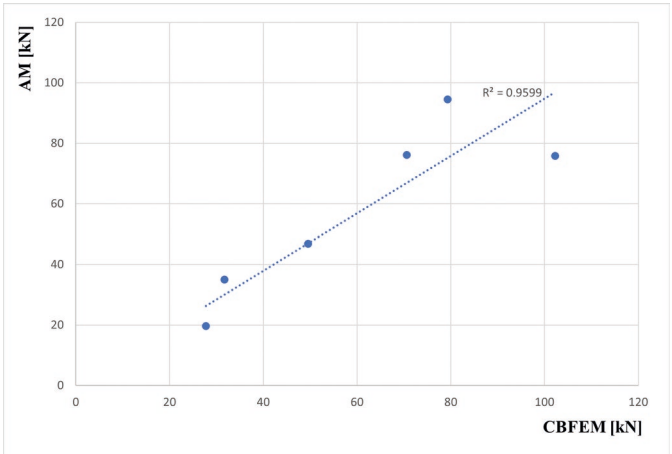

Fig. 7 Comparison of T-stub resistances between the AM and the CBFEM

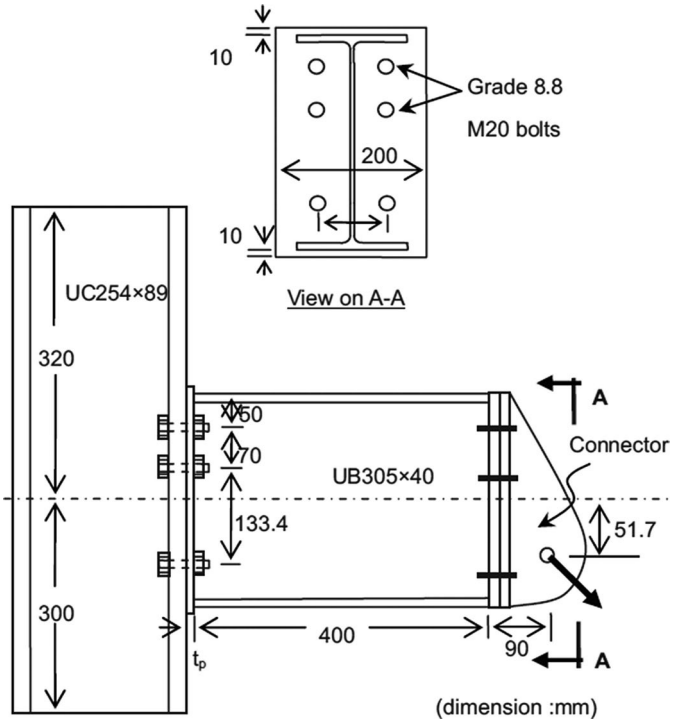

Fig. 8 The influence of the plastic limit strain at 450 °C

The nominal characteristics values of steel material properties are used to model the connections since the CBFEM is an NDC model. The study aims to provide accurate and safe results to structural fire engineers at the design level. The values for bolts are taken from the study [5]. Tab. 3 presents the material properties used in the CBFEM models to simulate Sheffield's test. The material properties defined in the following table are elastic modulus, yield strength, and ultimate strength for the beam, column, plate, and bolt. At elevated temperatures, these values are reduced by the reduction factors as stated in EN 1993-1-2 [11].

4.2 Load–deformation curves

The CBFEM models are generated using the IDEA StatiCa Connection [26] to simulate the behaviour of flush endplate connections at elevated temperatures. In the numerical model, the applied load is divided into its components using trigonometric equations as normal and shear force. In this section, Fig. 9–12 shows the comparison between the load–rotation curves obtained from the experimental study (solid lines) and the CBFEM (dashed lines)

Tab. 2 Preferred image formats and resolutions

Test specimen	Plate thickness [mm]	Number of rows	Temperature [°C]	Nominal load angle [°]
Test 2	10	3	450	35
Test 3	10	3	550	35
Test 4	10	3	650	35
Test 6	10	3	450	45
Test 7	10	3	550	45
Test 8	10	3	650	45
Test 9	10	3	20	55
Test 10	10	3	450	55
Test 11	10	3	550	55
Test 12	10	3	650	55
Test 13	8	3	20	35
Test 14	8	3	550	35
Test 15	15	3	550	35

Tab. 3 Preferred image formats and resolutions

Parts	Elastic modulus [MPa]	Yield strength [MPa]	Ultimate Strength [MPa]
Beams	210000	275	430
Columns	210000	355	490
Plates	210000	275	430
Bolts	206209	692	865

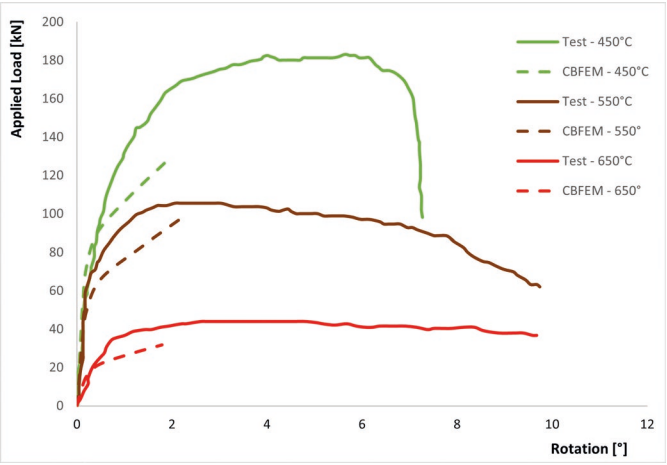

Fig. 9 The load–rotation graph, 35°

for different load angles. It is seen that the CBFEM predicts the ultimate resistance smaller than the measured ultimate resistance. For 35° and 45° loading angles, the load–deformation curves are not plotted at ambient temperature. Mostly, the CBFEM models developed load–deformation curves up to 2°. The experimental studies indicated that the increasing temperature leads to a significant drop in the resistance. The load angle also affects the connection resistance inversely at elevated temperatures. In Fig. 9, the results from the test and the CBFEM for the 35° loading angle are presented. At 35°, the load capacity of the flush endplate connections is underestimated by the CBFEM.

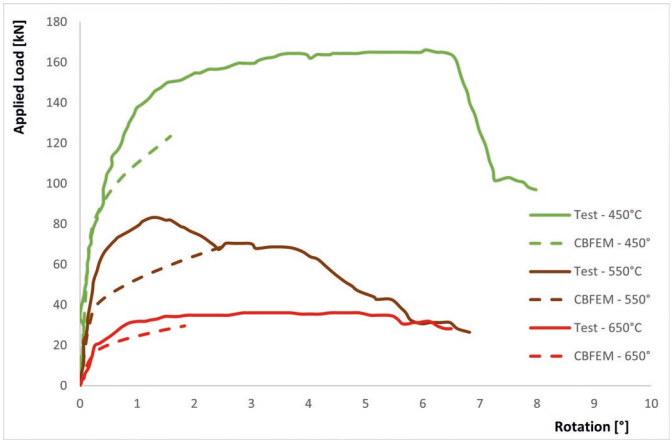

Fig. 10 The load–rotation graph, 45°

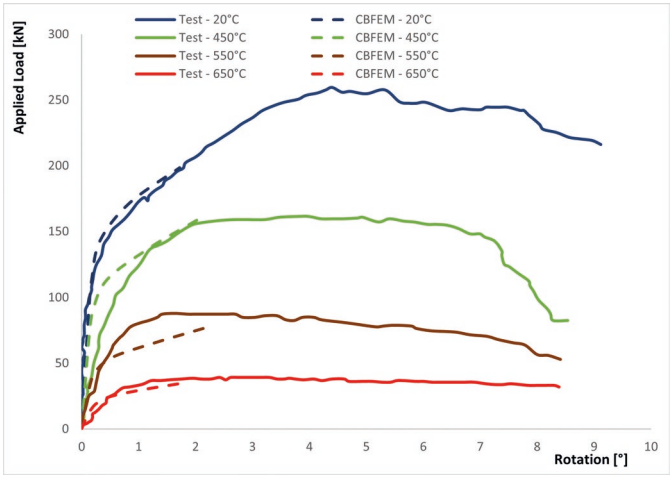

Fig. 11 The load–rotation graph, 55°

A comparison of the load–rotation response of the connection loaded with 45° is shown in Fig. 10. The plot displays two curves: one representing the experimental results from test results and the other showing the predictions from the CBFEM. It can be seen that the load–rotation response curves of the connection agree well with tests and the CBFEM model in the early stage. Further-

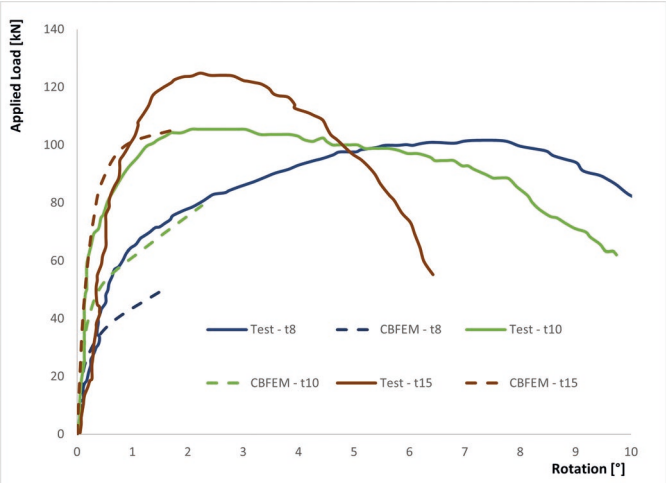

Fig. 12 The load–rotation graphs of different thickness plates at 550 °C

more, there exists a strong correlation between the initial stiffness derived from the CBFEM analysis and the results obtained through tests. The experimental results show a slightly earlier yielding point compared to the CBFEM predictions, reflecting a minor discrepancy in the initial response under higher loads. The ultimate load is very similar in both the experimental and numerical results, highlighting that the CBFEM model accurately predicts the maximum load the connection can withstand before failure.

The load–rotation behaviour of the tested connection, calculated by the CBFEM, is shown in Fig. 11 for ambient and elevated temperatures. It can be seen that there is a good correlation for rotations up to 2° between test results and calculated load–rotation behaviour. Both the experimental and CBFEM curves exhibit an initial linear response with similar slopes, indicating comparable initial stiffness. The yield point is well aligned between the CBFEM model and the experimental results, which suggests that the model effectively predicts the onset of yielding in the connection when loaded at 55°.

Fig. 12 illustrates the comparison of the load–rotation response of steel connections with varying endplate thicknesses at an elevated temperature of 550 °C. The stiffness of the connection is influenced by the thickness of the endplate. The CBFEM model closely follows the experimental results in capturing both the elastic and post-elastic behaviour of the connections. Increasing the thickness of endplates enhances the resistance of flush endplate connections; however, the ductility of the connections decreases.

CBFEM is a practical and design-oriented methodology used to ensure the safety and compliance of steel connections with structural codes, such as the Eurocode, particularly at elevated temperatures. While the results may not fully capture the actual behaviour observed in tests, they offer a robust framework for ensuring structural resilience, emphasizing safety over precision.

4.3 Failure modes

Authors from the experimental study reported that the test specimens with 10 mm plate thickness failed due to two failure modes [5]. Fracture of the endplate governs the failure mode of testes specimens at ambient and 450 °C. However, the bolts in the top row also have significant deformation, but no fracture is observed at 450 °C, as shown in Fig. 13. It can be seen that a small crack is developed during tests and the plastic strain on the beam web near weld equals limit strain.

At 550 and 650 °C, the top two bolts were completely fractured with high ductile behaviour and a moderate bending deformation occurred in the endplate. Fig. 14 indicates the endplate and bolts at 650 °C after failure and plastic strain distribution on the test specimen obtained from the CBFEM. As observed in the test, the CBFEM measures only 0.3 % plastic strain while the bolts in the top row reach their ultimate capacity.

The flush endplate connections using the endplate thickness of 8 mm are tested at ambient temperature and 550 °C. At room temperature, the endplate deformation leads to the failure of the test specimen. The bolts don't have significant deformation. Fig. 15 shows that the observed deformations of the connection components were followed by the CBFEM model at 550 °C. It can be observed that the failure is controlled by the bolt fracture. In CBFEM, the bolts at the top row reach 99.9 % capacity. Severe bending cycles occurred in the endplate and the plastic strain of the endplate equals 4.34 % which is close to the limit strain.

Tab. 4 lists the comparison of the failure modes from test results and the CBFEM models. In the CBFEM, the 5 %

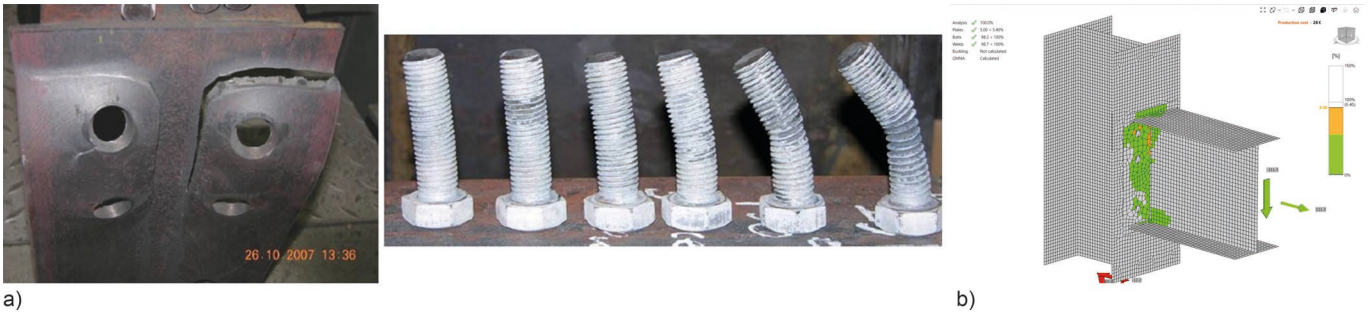

a) b)

Fig. 13 Deformed shape of the connection at 450 °C: a) test and b) CBFEM

a) b)

Fig. 14 Deformed shape of the connection at 650 °C: a) test and b) CBFEM

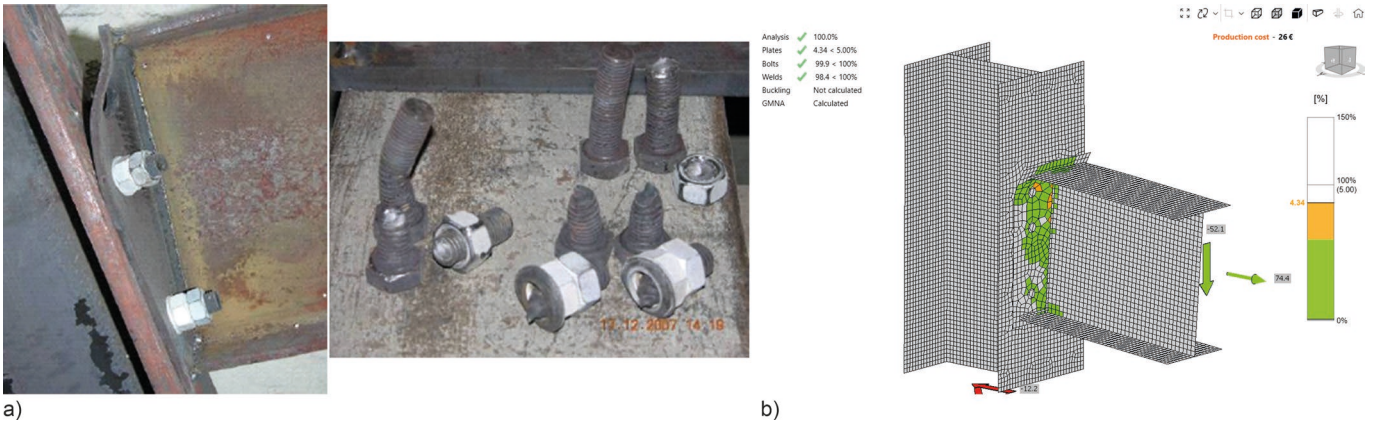

a) b)

Fig. 15 Deformed shape of the connection with 8 mm endplate at 550 °C: a) test and b) CBFEM

Tab. 4 Comparison of failure modes from the test [5] and the CBFEM model

Test specimen	**Test description**		**Failure modes**	
	Angle [°]	***T* [°C]**	**CBFEM**	**Test**
Test 2	35	450	5 % plastic strain on end-plate	Plate fracture
Test 3	35	550	100 % bolt capacity	Bolt fracture
Test 4	35	650	100 % bolt capacity	Bolt fracture
Test 6	45	450	5 % plastic strain on end-plate	Plate fracture
Test 7	45	550	100 % bolt capacity	Bolt fracture
Test 8	45	650	100 % bolt capacity	Bolt fracture
Test 9	55	20	5 % plastic strain on end-plate	Plate fracture
Test 10	55	450	100 % bolt capacity	Plate fracture
Test 11	55	550	100 % bolt capacity	Bolt fracture
Test 12	55	650	100 % bolt capacity	Bolt fracture
Test 13	35	20	5 % plastic strain on end-plate	Plate fracture
Test 14	35	550	100 % bolt capacity	Bolt fracture
Test 15	35	650	100 % bolt capacity	Bolt fracture

plastic strain on the endplate means that failure occurs in the endplate. Meanwhile, if the bolt capacity reaches 100 % capacity before steel plates have 5 % plastic strain, the connection fails due to bolt failure. The capacity of bolts is calculated using the equations for bolts in tension, shear, and bearing according to Eurocode. As shown in Tab. 4, the CBFEM models predicted the same failure modes for all test specimens as observed during the experimental study. However, one notable exception was observed in Test 10, where the failure mode differed between the CBFEM prediction and the experimental results. While the CBFEM model predicted a failure due to 100% bolt capacity, the experiment revealed plate fracture as the actual failure mechanism. Although the load–deformation curves indicated that the resistance is changing according to the loading angle, there is no influence on the failure modes of flush endplate connections.

Fig. 16 compares resistance values obtained from CBFEMs and experiments, with an R^2 value of 0.9136. This value indicates a good correlation between the CBFEM predictions and the measured results. The

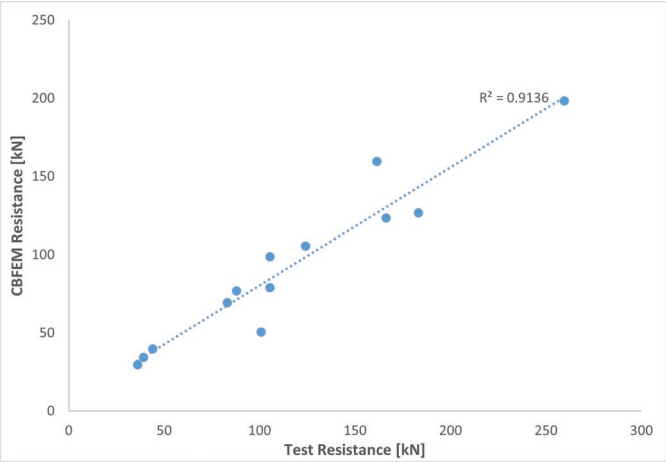

Fig. 16 Comparison of resistance predicted by the CBFEM model and experimentally measured resistance

R_{CBFEM}/R_{Test} ratio ranges from 0.5 (Test 13) to 0.99 (Test 10), indicating varying levels of agreement between CBFEM predictions and experimental results. On average, the ratio is ≈0.81, meaning the CBFEM model generally underestimates resistance by about 19%.

5 Parametric studies

Parametric studies for finite-element models are performed to investigate the sensitivity of the model and its responses to variations in key parameters. The investigated parameters are plastic limit strain, bolt elongation, and bolt diameter. The specimens from Test 6 and Test 8 are selected for parametric studies since two different failures were observed.

5.1 Effect of plastic limit strain

To investigate the influence of the plastic limit strain which is recommended in EN 1993-1-5 [22] on the load–rotation curves of flush endplate connections at 450 and 650 °C, the plastic limit strain varies from 5 to 15 %. Increasing the plastic limit strain of steel plates does not change the trend of the load–rotation curve; however, the rotation capacity is increased from 2.26° to 3.7° at 450 °C as seen in Fig. 17. Fig. 18 illustrates the effect of plastic limit strain on steel connections subjected to a temperature of 650 °C. The 5 % plastic limit strain leads to higher resistance of steel connections; however, the connection is not able to reach the rotational capacity as obtained using 10 and 15 % plastic limit strain. The use of higher plastic limit strain in steel significantly enhances the rotational capacity of steel connections, especially at elevated temperatures such as 650 °C.

5.2 Effect of bolt elongation

ISO 898 [25] proposes the values of bolt elongation for different bolt types at ambient temperature. The CBFEM uses these values to prepare the load–deformation model

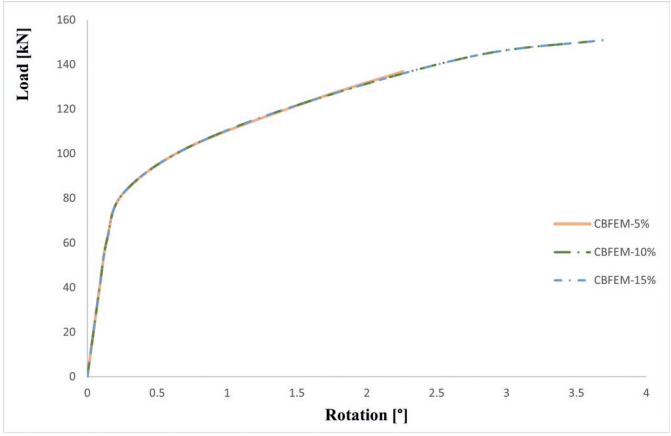

Fig. 17 The influence of the plastic limit strain at 450 °C

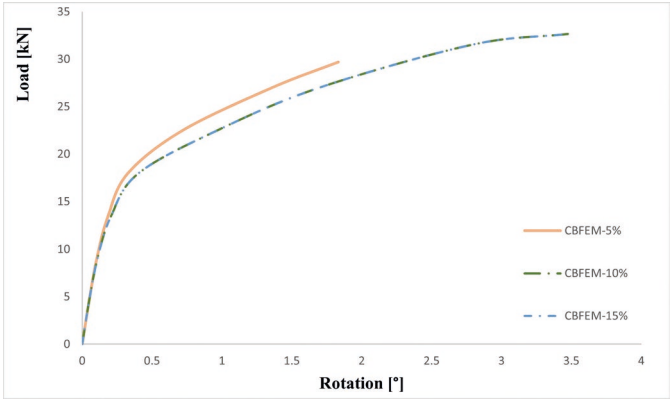

Fig. 18 The influence of the plastic limit strain at 650 °C

for bolts to model the bolted connection. Furthermore, the test results showed that the bolt behaviour is highly ductile at elevated temperatures. Therefore, the influence of bolt elongation on the mechanical response of the tested connections is analysed by varying the bolt elongation from 12 % to 20 %. The results of the CBFEM in terms of load–rotation curves for each value of the bolt elongation are depicted in Figs. 19 and 20. Fig. 19 shows that the bolt elongation does not have a significant effect on the connection behaviour if the connections fail due to the plate fracture. While the bolt elongation is increased, the resistance of the connection is decreased with higher rotation capacity. As the bolt elongation increases, the

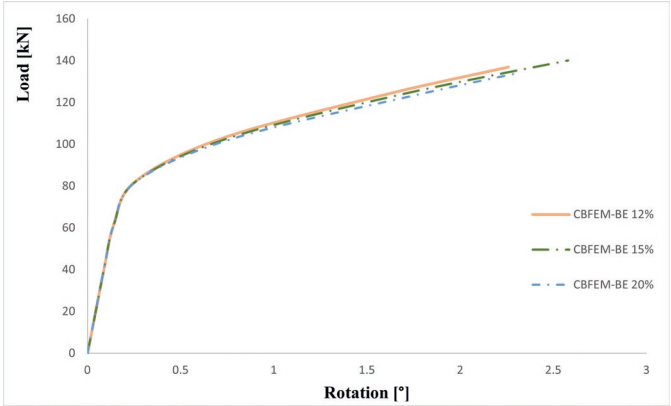

Fig. 19 The influence of the bolt elongation at 450 °C

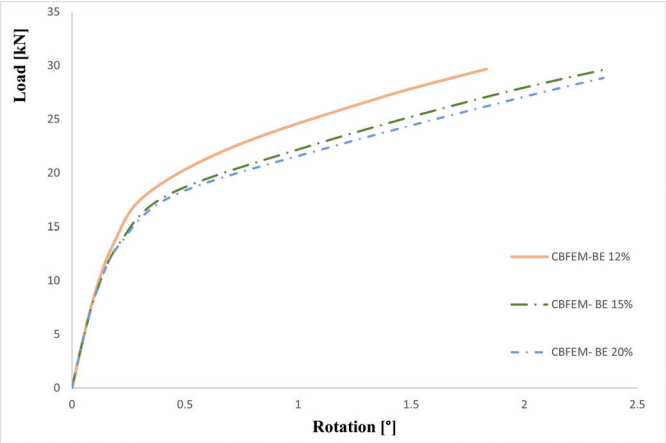

Fig. 20 The influence of the bolt elongation at 650 °C

connection's resistance is reduced, accompanied by an enhanced rotation capacity, as depicted in Fig. 20.

5.3 Effect of bolt diameter

Clearly, the bolt diameter also plays an important role in the behaviour of the analysed connections at elevated temperatures. In fact, the increase in the bolt diameter results in a progressive increase in the connection resistance. Conversely, the decrease in the bolt diameter leads to an increase in the connection rotation capacity at 450 and 650 °C, as shown in Figs. 21 and 22.

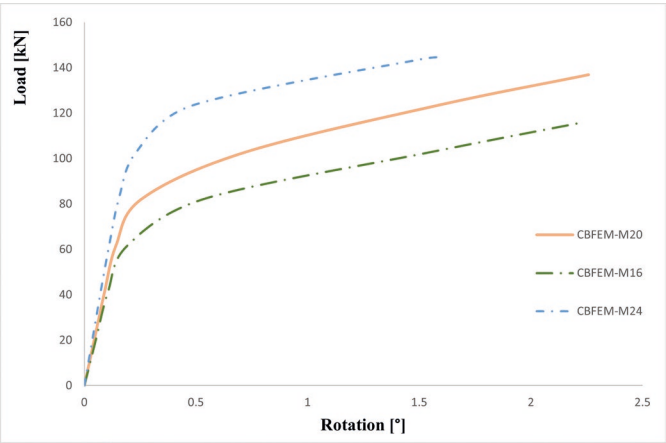

Fig. 21 The influence of the bolt diameter at 450 °C

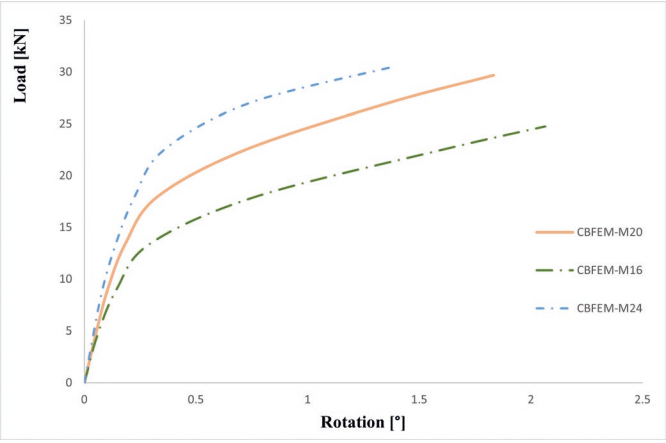

Fig. 22 The influence of the bolt diameter at 650 °C

6 Conclusions

The CBFEM model was generated to develop NDC for flush endplate connections at elevated temperatures. The CBFEM model is validated based on test results from literature and is verified against Eurocode design specifications. Then, the parametric studies were employed to assess the influence of key parameters on the behaviour of flush endplate connections at elevated temperatures.

The experimental and numerical plots demonstrated that the NDC models may predict the bolted connection behaviour at both ambient and elevated temperatures. It was also observed that, with only one exception, the connections both in the CBFEM models and in the experiments failed by the same failure modes. The characteristics of load–rotation curves, developed by the CBFEM, are relatively in good agreement with measured test data. Since the goal is safe design rather than precise modelling, CBFEM often yields conservative predictions compared to experimental test results. This approach ensures that connections are designed to deal with fire severity aligning with established standards. The CBFEM model was verified by comparing the resistance of the T-stub specimens calculated from Eurocode equations. The coefficient of determination was evaluated as 0.95. It can be concluded that the CBFEM is a reliable method to design bolted connections compared to AM. The parametric study investigated the effect of three parameters on the load–deformation curves. The results stated that the most effective parameter on the behaviour of flush endplate connections at elevated temperatures was the bolt diameter. The primary conclusions from this research are as follows.

- The developed CBFEM model is able to evaluate the mechanical response of flush endplate connections subjected to different loading conditions at elevated temperatures.
- Since the CBFEM provided smaller resistance values than test results and predicted the same failure mode as observed in tests, it may be utilized as a design tool for structural fire engineers.
- The verification study highlighted that the CBFEM is a reliable model for designing bolted connections at elevated temperatures.
- The recommended 5 % plastic limit strain for steel plates can be also used for the fire design of steel connections.

In future studies, the effects of temperature variations within connection components will be investigated to simulate more realistic scenarios compared to the theoretical approach. These temperature differences can significantly influence the capacity of steel connections under elevated temperature conditions.

References

[1] Wald, F.; Sokol, Z.; Moore, D. (2009) *Horizontal forces in steel structures tested in fire.* Journal of Constructional Steel Research 65, No. (8–9), pp. 1896–1903. https://doi.org/10.1016/j.jcsr.2009.04.020

[2] Tran, V.-L.; Kim, S.-E. (2022) *Rapid prediction of the ultimate moment of flush endplate connections at elevated temperatures through an artificial neural network.* Expert Systems with Applications 206, p. 117759. https://doi.org/10.1016/j.eswa.2022.117759

[3] Elkady, A. (2022) *Response characteristics of flush end-plate connections.* Engineering Structures 269, p. 114856, https://doi.org/10.1016/j.engstruct.2022.114856

[4] Jones, L. C. L.; Burgess, I. W.; Lennon, T.; Plank, R. J. (1997) *Elevated-temperature moment-rotation tests on steelwork connections.* Proceedings of the Institution of Civil Engineers Structures and Buildings 122, pp. 410–419. https://doi.org/10.1680/istbu.1997.29830

[5] Yu, H.; Burgess, I. W.; Davison, J. B.; Plank, R. J. (2011) *Experimental and numerical investigations of the behavior of flush end plate connections at elevated temperatures.* Journal of Structural Engineering 137, No. (1), pp. 80–87. https://doi.org/10.1061/(ASCE)ST.1943-541X.0000277

[6] Li, J. T.; Li, G. Q.; Lou, G. B. (2012) *Experimental investigation on flush end-plate bolted composite connection in fire.* Journal of Constructional Steel Research 76, pp. 121–132. https://doi.org/10.1016/j.jcsr.2012.03.022

[7] Ataei, A.; Bradford, M. A.; Valipour, H. R. (2015) *Experimental study of flush end plate beam-to-CFST column composite joints with deconstructable bolted shear connectors.* Engineering Structures 99, pp. 616–630. https://doi.org/10.1016/j.engstruct.2015.05.012

[8] Khonsari, S. V.; Nejati, S.; Rahdan, M.; Ahmadi, M. (2023) *Behaviour of thin flush end-plate connections in a 3D bare steel frame under fire loading: experimental study.* Journal of Structural Fire Engineering 14 No. 1, pp. 15–33. https://doi.org/10.1108/JSFE-08-2021-0050

[9] Lu, P.; Yang, J. J.; Ran, T.; Wang, W. Y. (2023) *Experimental study on flexural capacity and fire resistance of high strength Q690 steel flush end-plate connections.* Thin-Walled Structures 184, p. 110506. https://doi.org/10.1016/j.tws.2022.110506

[10] CEN (2006) *EN 1993-1-8, Eurocode 3: Design of steel structures, Part 1-8: Design of joints.* Brussels, Belgium: European Committee for Standardisation.

[11] CEN. (2006) EN 1993-1-2, *Eurocode 3: Design of steel structures, Part 1-2: General rules, structural fire design.* Brussels, Belgium: European Committee for Standardisation.

[12] Gernay, T. (2024) *Performance-based design for structures in fire: Advances, challenges, and perspectives.* Fire Safety Journal 142, p. 104036. https://doi.org/10.1016/j.firesaf.2023.104036

[13] Al-Jabri, K.; Seibi, A.; Karrech, A. (2006) *Modelling of unstiffened flush end-plate bolted connections in fire.* Journal of Constructional Steel Research 62, No. (1–2), pp. 151–159. https://doi.org/10.1016/j.jcsr.2005.04.016

[14] Shrih, A.; Rahman, A.; Al-Jabri, K. S. (2009) *Finite element analyses of flush end-plate connections between steel beams and columns at elevated temperatures.* Advances in Structural Engineering 12, No. 3, pp. 311–324. https://doi.org/10.1260/136943309788708365

[15] Schaumann, P.; Kirsch, T. (2013) *Simulation of a flush endplate connection at elevated temperatures including fracture simulation.* Journal of Structural Fire Engineering 4, No. 2, pp. 103–112. https://doi.org/10.1260/2040-2317.4.2.103

[16] Tran, V.-L. (2020) *Moment-rotation-temperature model of semi-rigid cruciform flush endplate connection in fire.* Fire Safety Journal 114, p. 102992. https://doi.org/10.1016/j.firesaf.2020.102992

[17] Wang, W.; Li, S.; Ran, T. (2024) *Numerical study on high strength q690 steel flush end-plate connections at elevated temperatures.* Fire Technology 60, pp. 3269–3294. https://doi.org/10.1007/s10694-024-01568-y

[18] CEN. (2021) *prEN 1993–1-14:2021, Eurocode 3: Design of steel structures, Part 1-14: Design assisted by finite element analysis.* Brussels, Belgium: European Committee for Standardisation.

[19] Der, B.; Wald, F., (2024) *Numerical design calculation of bolted lap joints at elevated temperatures.* Fire Safety Journal 147, p. 104202. https://doi.org/10.1016/j.firesaf.2024.104202

[20] Der, B.; Wald, F.; Vild, M. (2024) *Numerical design calculation of fin plate connections in fire.* Proceedings of the 7th International Conference on Geotechnics, Civil Engineering and Structures, CIGOS 2024, Ho Chi Minh City, Vietnam, 4–5 April. Lecture Notes in Civil Engineering, Vol. 482. Springer: Singapore. https://doi.org/10.1007/978-981-97-1972-3_60

[21] Der, B.; Wald, F.; Vild, M. (2024) *Numerical design calculation of T-stubs at elevated temperatures.* Fire Technology 61, pp. 541–562, https://doi.org/10.1007/s10694-024-01626-5

[22] CEN (2006) *EN 1993-1-5*, *Eurocode 3: Design of steel structures, Part 1-5: General rules – plated structural elements.* Brussels, Belgium: European Committee for Standardisation.

[23] Verein Deutscher Ingenieure (2003) *Systematic calculation of high duty bolted joints joints with one cylindrical bolt.* VDI-Handbuch Konstruktion.

[24] Agerskov, H. (1976) *High-strength bolted connections subject to prying.* Journal of Structural Division, ASCE 102, pp. 161–175. https://doi.org/10.1061/JSDEAG.0004253

[25] ISO 898–1 (2009) *Mechanical properties of fasteners made of carbon steel and alloy steel, Part 1, Bolts, screws and studs with specified, property classes, Coarse thread and fine pitch thread.* Geneva.

[26] IDEA StatiCa Connection (2023) *Theoretical background* [online]. https://resources.ideastatica.com (accessed on: 10 Oct. 2024)

[27] Wald F., Kwasniewski L., Gödrich L., Kurejková M. (2014) *Validation and verification procedures for connection design in steel structures.* 12th International conference on steel, space and composite structures. pp. 111–120.

[28] SCI (2002) *Joints in steel connection, Simple connections.* The Steel Construction Institute and The British Constructional Steelwork Association Limited: UK.

Authors
Batuhan Der, Ph.D. (corresponding author)
batuhan.der@unitn.it
Università degli Studi di Trento
Dipartimento di Ingegneria Civile
Ambientale e Meccanica
Via Mesiano 77
38123 Trento, TN
Italy

Prof. Ing. C.Sc. František Wald
wald@fsv.cvut.cz
Czech Technical University in Prague
Department of Steel & Timber Structures
Thákurova 2077/7, 160 00 Praha 6 – Dejvice
Czech Republic

Dr. Martin Vild
martin.vild@vutbr.cz
Institute of Metal and Timber Structures
Brno University of Technology
Veveri 95
60200 Brno
Czech Republic

How to Cite this Paper
Der, B.; Wald, F.; Vild, M. (2025) *Numerical design calculation of flush endplate connections at elevated temperatures*. Steel Construction 18, No. 2, pp. 121–133.
https://doi.org/10.1002/stco.202400043

This paper has been peer reviewed. Submitted: 09. October 2024; accepted: 24. February 2025.